Eur. Phys. J. C 54, 277–284 (2008)
DOI 10.1140/epjc/s10052-007-0520-3

THE EUROPEAN PHYSICAL JOURNAL C

Regular Article – Theoretical Physics

The role of beam polarization for radiative neutralino production at the ILC

H.K. Dreiner, O. Kittel, U. Langenfeld[a]

Physikalisches Institut der Universität Bonn, Nußallee 12, 53115 Bonn, Germany

Received: 21 June 2007 / Revised version: 2 November 2007 /
Published online: 24 January 2008 –

Abstract. We analyze the impact of electron and positron beam polarization on radiative neutralino production at the international linear collider (ILC). We focus on three different mSUGRA scenarios in turn at the Higgs strahlung threshold, the top pair production threshold, and at $\sqrt{s} = 500\,\text{GeV}$. In these scenarios at the corresponding $\sqrt{s}$, radiative neutralino production is the only supersymmetric production mechanism that is kinematically allowed. The heavier neutralinos and charginos as well as the sleptons, squarks and gluinos are too heavy to be pair produced. We calculate the signal cross section and also the standard model background from radiative neutrino production. For our scenarios, we obtain significances larger than 10 and signal to background ratios between 2% and 5%, if we have electron beam polarization $P_{e^-} = 0.0$–0.8 and positron beam polarization $P_{e^+} = 0.0$–0.3. If we have electron beam polarization of $P_{e^-} = 0.9$, then the signal is observable with $P_{e^+} = 0.0$ but both the significance and the signal to background ratio are significantly improved for $P_{e^+} = 0.3$.

1 Introduction

The minimal supersymmetric standard model (MSSM) is a promising extension of the standard model of particle physics (SM) [1–4]. If weak scale supersymmetry (SUSY) exists, it should be discovered at the LHC [5], which is scheduled to start in 2008. However, detailed measurements of the masses, decay widths, couplings, and spins of the discovered particles are only possible at the international linear collider (ILC) [5–9]. In the first stage of the ILC, the center-of-mass energy will be $\sqrt{s} = 500\,\text{GeV}$, and the luminosity, $\mathcal{L}$, will be $500\,\text{fb}^{-1}$ within the first four years.

In preparing for the ILC, there is an on-going debate over the extent of beam polarization to be included in the initial design [6, 10–13]. It is clear that there will be at least 80% polarization of the electron beam, possibly even 90% [14]. A polarized positron beam is technically and financially more involved. However, it is possible to achieve 30% polarization through the undulator based production of the positrons, already from the start [13]. Depending on the undulator length, even a higher degree of positron polarization can be achieved. In light of this discussion, it is the purpose of this letter to reconsider the effect of various degrees of electron and positron polarization on a particular supersymmetric production process, namely the radiative production of the lightest neutralino mass eigenstate $\tilde{\chi}_1^0$

$$e^+ + e^- \to \tilde{\chi}_1^0 + \tilde{\chi}_1^0 + \gamma\,. \tag{1}$$

We shall focus on specific regions of the supersymmetric parameter space. The signal is a single, highly energetic photon and missing energy, carried by the neutralinos.

The process (1) was previously studied within the MSSM and with general neutralino mixing in [15–17]. The additional effect of polarized beams was considered in [18–20]. In [18], it was shown that polarized beams significantly enhance the signal and simultaneously suppress the main SM photon background from radiative neutrino production,

$$e^+ + e^- \to \nu + \bar{\nu} + \gamma\,. \tag{2}$$

Moreover, it was pointed out that for certain regions of the MSSM parameter space, the process (1) is kinematically the *only* accessible SUSY production mechanism in the first stage of the ILC at $\sqrt{s} = 500\,\text{GeV}$ [18]. Here the heavier electroweak gauginos and the sleptons are too heavy to be pair produced, i.e. their masses are above 250 GeV.

Other than the standard center-of-mass energy, $\sqrt{s} = 500\,\text{GeV}$, at the ILC, also lower energies are of particular interest, namely for Higgs and top physics. Higgs strahlung,

$$e^+ + e^- \to Z + h\,, \tag{3}$$

can be well studied at the threshold energy $\sqrt{s} = m_h + m_Z$, which is $\sqrt{s} \approx 220\,\text{GeV}$, for a Higgs boson mass of $m_h \approx 130\,\text{GeV}$. The CP quantum number and the spin of the Higgs boson can be determined from an energy scan of the production cross section near the threshold [23].

[a] e-mail: ulrich@th.physik.uni-bonn.de

From a scan at the threshold energy of top pair production, $\sqrt{s} = 2m_t \approx 350\,\text{GeV}$, the top mass m_t can be determined with an error $\delta m_t < 0.1\,\text{GeV}$ [6]. Thus the present error on the top mass, $\delta m_t \approx 3\,\text{GeV}$ [24], and the foreseen error from LHC measurements, $\delta m_t \approx 1\,\text{GeV}$ [25], can be reduced by one order of magnitude. Also the top width, Γ_t, and the strong coupling constant, α_s, can be precisely determined by a multi parameter fit of the cross section, top momentum distribution, and forward–backward charge asymmetry near threshold [26].

In this letter, we take these physics questions as a motivation to study the role of polarized beams in radiative neutralino production at the energies $\sqrt{s} = 220\,\text{GeV}$, 350 GeV, and 500 GeV at the ILC. For each beam energy, we shall focus on a specific supersymmetric parameter set within the context of minimal supergravity grand unification (mSUGRA) [21, 22]. We thus consider three mSUGRA scenarios, which we label A, B and C, respectively, and which are listed below in Table 1 together with the resulting spectra in Table 2. We restrict ourselves to mSUGRA scenarios, in order to reduce the number of free parameters and since we find it sufficient to illustrate our point. The specific scenarios are chosen such that radiative neutralino production is the *only* supersymmetric production mechanism which is kinematically accessible at the given center-of-mass energy. It is thus of particular interest to learn as much about supersymmetry as is possible through this mechanism. As we shall see, beam polarization is very helpful in this respect.

In Sect. 2, we define the significance, the signal to background ratio and define a first set of experimental cuts. In Sect. 3, we study numerically the dependence of the signal cross section and the SM background, the significance, and the signal to background ratio on the beam polarization. In particular, we compare the results for different sets of beam polarizations, $(P_{e^+}|P_{e^-}) = (0|0)$, $(0|0.8)$, $(-0.3|0.8)$, $(-0.6|0.8)$, $(0|0.9)$ and $(-0.3|0.9)$. We summarize and conclude in Sect. 4.

Table 1. Definition of the mSUGRA scenarios A, B, and C. All values are given in GeV. We have fixed $\tan\beta = 10$. For completeness we have included the corresponding value of $\sqrt{s}$ for each scenario

Scenario	$\sqrt{s}$	M_0	$M_{1/2}$	A_0	M_1	M_2	μ
A	220	90	225	−90	97.5	188	316
B	350	135	325	−135	143	272	444
C	500	200	415	−200	184	349	560

Table 2. Spectrum of the lighter SUSY particles for scenarios A, B, and C, calculated with SPheno [32]. All values are given in GeV. For completeness we have included the corresponding value of $\sqrt{s}$ for each scenario

Scenario	$\sqrt{s}$	$m_{\chi_1^0}$	$m_{\chi_2^0}$	$m_{\chi_1^\pm}$	$m_{\tilde{\tau}_1}$	$m_{\tilde{e}_R}$	$m_{\tilde{e}_L}$	$m_{\tilde{\nu}}$
A	220	92.4	172	172	124	133	189	171
B	350	138	263	263	183	191	270	258
C	500	180	344	344	253	261	356	347

2 Definitions and cuts

We wish to study the beam polarization dependence of the cross sections for the signal process (1) and the background process (2). In the following, we define the theoretical significance as [18]

$$S = \frac{\sigma_{\text{Signal}}}{\sqrt{\sigma_{\text{Signal}} + \sigma_{\text{Background}}}}\sqrt{\mathcal{L}}\,, \tag{4}$$

and the signal to background ratio (or reliability) as [18]

$$r = \frac{\sigma_{\text{Signal}}}{\sigma_{\text{Background}}}\,. \tag{5}$$

Here σ_{Signal} and $\sigma_{\text{Background}}$ shall refer to the signal and background cross sections also after the cuts we impose on the final state phase space. A significance of $S = 1$ implies that the signal can be measured at the statistical 68%-level. If the experimental error for the background is, for example, 1%, the signal to background ratio must be greater than 1% [29, 30]. For a signal to be detectable at the ILC requires at least

$$S > 1 \quad \text{and} \quad r > 1\%\,. \tag{6}$$

We remark that these criteria can only be seen as rough estimates to judge whether an excess of signal photons can be measured over the background, since we do not include any detector simulation, with effective particle reconstruction efficiencies. A detailed Monte Carlo study is beyond the scope of the present work.

For the tree-level calculation of the cross sections, we use the formulæ for the amplitudes squared as given in [18], where details of the neutralino mixing can also be found. To regularize the infrared and collinear divergences of the tree-level cross sections for signal and background, we apply cuts on the photon scattering angle θ_γ [18]

$$|\cos\theta_\gamma| \leq 0.99\,, \tag{7}$$

and on the photon energy E_γ [18]

$$0.02 \leq x \leq 1 - \frac{m_{\chi_1^0}^2}{E_{\text{beam}}^2}\,, \quad x = \frac{E_\gamma}{E_{\text{beam}}}\,, \tag{8}$$

with the beam energy $E_{\text{beam}} = \sqrt{s}/2$. The upper cut on the photon energy $x^{\max} = 1 - m_{\chi_1^0}^2/E_{\text{beam}}^2$ is the kinematical limit of radiative neutralino production, and it also reduces much of the on-shell Z boson contribution to the background from radiative neutrino production [18]. We assume that the mass of the lightest neutralino $m_{\chi_1^0}$ is known from LHC measurements [5]. Although $m_{\chi_1^0}$ can be measured at the percent-level at the LHC, such a precision will not be required for the upper cut $x^{\max}$, since the endpoint of the photon energy distribution is not densely populated with signal events. Finally, note that the ratios S

and r only weakly depend on the absolute values of the cuts $|\cos\theta_\gamma| \leq 0.99$, and $0.02 \leq x$, since signal and background have similar distributions in energy E_γ and angle θ_γ [18].

3 Numerical results

We define three mSUGRA scenarios A, B, and C for the three different energies $\sqrt{s} = 220\,\text{GeV}$, 350 GeV, and 500 GeV, respectively; see Table 1. We choose the three scenarios in such a way, that only the lightest neutralinos can be radiatively produced for each of the $\sqrt{s}$ values, respectively. The other SUSY particles, i.e. the heavier neutralinos and charginos, as well as the sleptons and squarks are too heavy to be pair produced at the ILC. It is thus of paramount interest to have an optimal understanding of the signature (1), in order to learn as much as possible about SUSY at a given ILC beam energy. Note that in the three scenarios (A, B, C) the squark and gluino masses are below $\{600, 800, 1000\}$ GeV, respectively, and should be observable at the LHC [5].

Scenario A is related to the Snowmass point SPS1a [27,28,31] by scaling the common scalar mass M_0, the unified gaugino mass $M_{1/2}$, and the common trilinear coupling A_0 by 0.9. Thus the slope $M_0 = -A_0 = 0.4\,M_{1/2}$ remains unchanged. For scenarios B and C, we also choose $M_0 = -A_0$; however, we change the slopes to $M_0 = 0.42\,M_{1/2}$ in scenario B, and $M_0 = 0.48\,M_{1/2}$ in scenario C. For all scenarios, we fix the ratio $\tan\beta = 10$ of the vacuum expectation values of the two neutral Higgs fields. In Table 1, we explicitly give the relevant low energy mSUGRA parameters for all scenarios. These are the U(1) and SU(2) gaugino mass parameters M_1 and

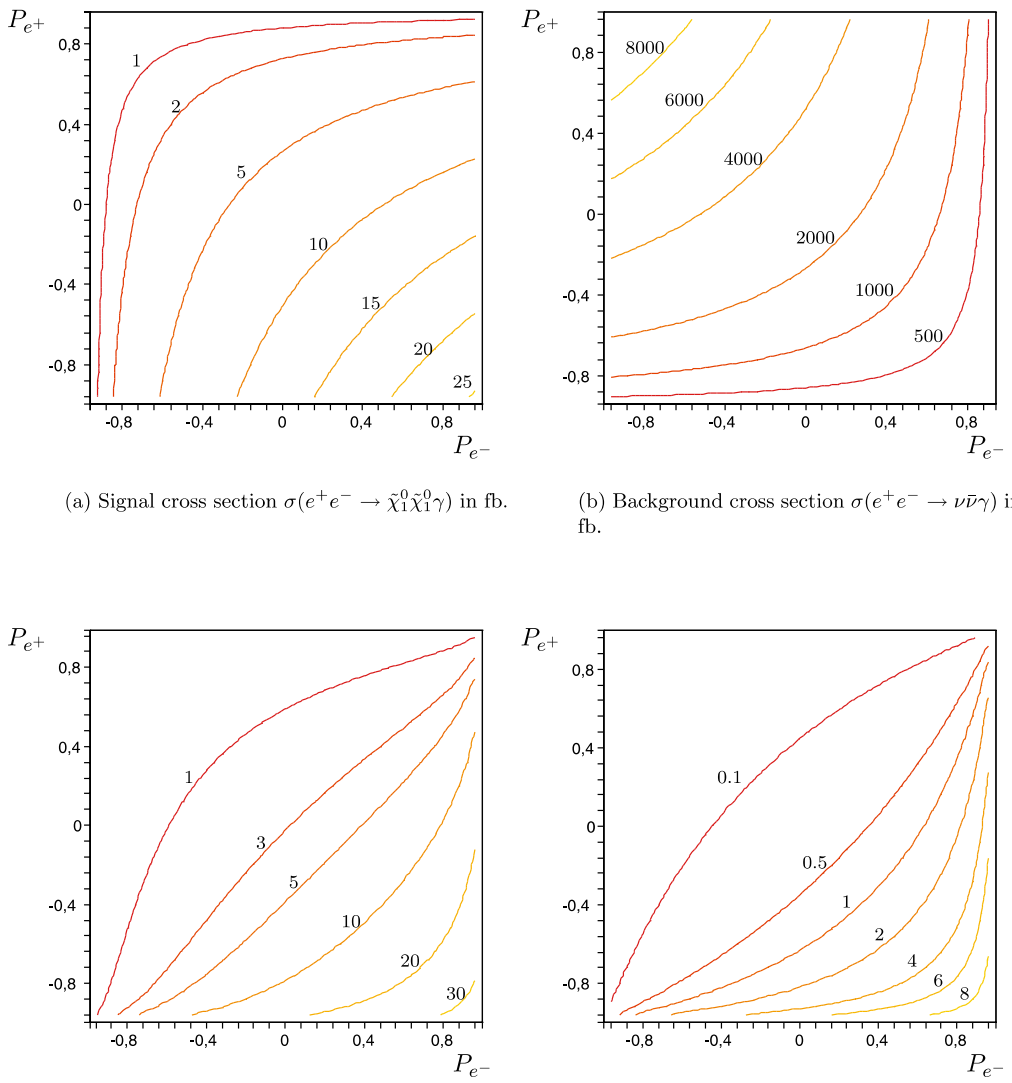

(a) Signal cross section $\sigma(e^+e^- \to \tilde{\chi}_1^0\tilde{\chi}_1^0\gamma)$ in fb.

(b) Background cross section $\sigma(e^+e^- \to \nu\bar{\nu}\gamma)$ in fb.

(c) Significance S.

(d) Signal to background ratio r in %.

Fig. 1. Signal cross section **a**, background cross section **b**, significance **c**, and signal to background ratio **d** for $\sqrt{s} = 220$ GeV, and an integrated luminosity $\mathcal{L} = 500\,\text{fb}^{-1}$ for scenario A: $M_0 = 90$ GeV, $M_{1/2} = 225$ GeV, $A_0 = -90$ GeV, and $\tan\beta = 10$; see Tables 1 and 2

M_2, respectively, and the higgsino mass parameter μ. The masses of the light neutralinos, charginos, and sleptons are given in Table 2. All parameters and masses are calculated at one-loop order with the computer code SPheno [32].

Note that the lightest neutralino, $\tilde{\chi}_1^0$, is mostly bino in all three scenarios; 98% in scenario A, 99.1% in scenario B, and 99.5% in scenario C. Thus in our scenarios, radiative neutralino production proceeds mainly via right selectron exchange in the t and u channel. Left selectron exchange and Z boson exchange are severely suppressed [18]. The background process $e^+e^- \to \nu\bar{\nu}\gamma$ mainly proceeds via W boson exchange. Thus positive electron beam polarization $P_{e^-} > 0$ and negative positron beam polarization $P_{e^+} < 0$ should enhance the signal rate and reduce the background at the same time [18, 19]. This effect is clearly observed in Figs. 1–3 for all scenarios. The signal cross section and the background vary by more than one order of magnitude over the full polarization range.

For scenario A, we show the beam polarization dependence of the signal cross section $\sigma\big(e^+e^- \to \tilde{\chi}_1^0\tilde{\chi}_1^0\gamma\big)$ in Fig. 1a, and the dependence of the background cross section $\sigma(e^+e^- \to \nu\bar{\nu}\gamma)$ in Fig. 1b. In both cases we have implemented the cuts of (7) and (8). The contour lines in the P_{e^-}–P_{e^+} plane of the significance S, (4), and the signal to background ratio r, (5), are shown in Fig. 1c and d respectively. The results for scenario B are shown in Fig. 2, and those for scenario C are shown in Fig. 3.

In order to quantify the behavior, we give the values for the signal and background cross sections, the significance S and the signal to background ratio r for a specific set of beam polarizations $(P_{e^+}|P_{e^-}) = (0|0)$, $(0|0.8)$, $(-0.3|0.8)$, $(-0.6|0.8)$, $(0|0.9)$, and $(-0.3|0.9)$ in Tables 3–5 for the scenarios A, B, and C, respectively. In the tables, we also give

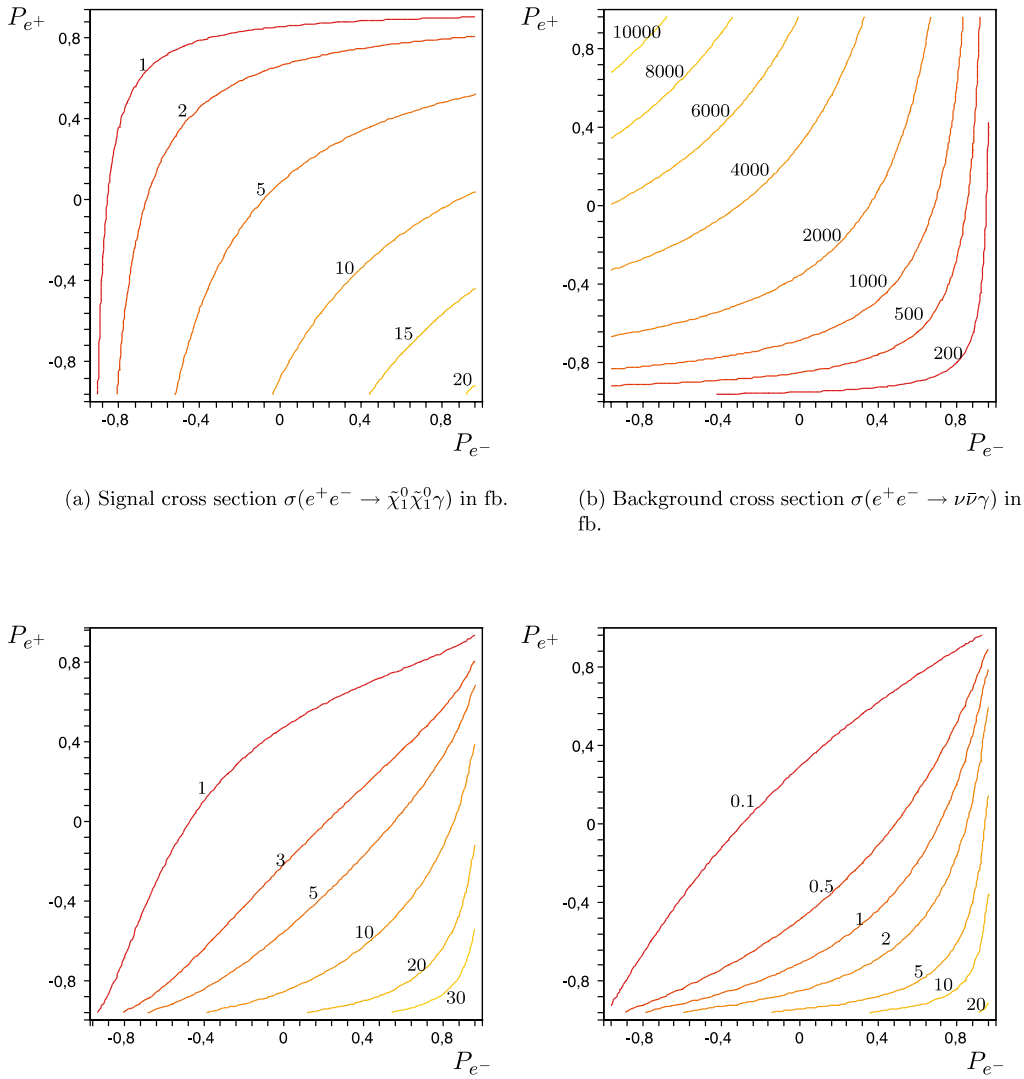

(a) Signal cross section $\sigma(e^+e^- \to \tilde{\chi}_1^0\tilde{\chi}_1^0\gamma)$ in fb.

(b) Background cross section $\sigma(e^+e^- \to \nu\bar{\nu}\gamma)$ in fb.

(c) Significance S.

(d) Signal to background ratio r in %.

Fig. 2. Signal cross section **a**, background cross section **b**, significance **c**, and signal to background ratio **d** for $\sqrt{s} = 350\,\text{GeV}$, and an integrated luminosity $\mathcal{L} = 500\,\text{fb}^{-1}$ for scenario B: $M_0 = 135\,\text{GeV}$, $M_{1/2} = 325\,\text{GeV}$, $A_0 = -135\,\text{GeV}$, and $\tan\beta = 10$; see Tables 1 and 2

the values for the effective beam polarization

$$P_{\rm eff} = \frac{P_{e^-} - P_{e^+}}{1 - P_{e^-} P_{e^+}}\,, \tag{9}$$

which is a helpful quantity for discussing combined polarizations when the electron and the positron beam polarizations have the opposite sign. For example, a double beam polarization of $P_{e^-} = 0.8$ and $P_{e^+} = -0.3$ acts effectively as (approximately) $P_{e^-} = 0.89$ of single beam polarization [33]. We find that an additional positron polarization $P_{e^+} = -30\%$ enhances the significance S by factors $\{1.5, 1.5, 1.6\}$ in scenarios $\{\mathrm{A}, \mathrm{B}, \mathrm{C}\}$, respectively, compared to beams with only e^- polarization $(P_{e^+}|P_{e^-}) = (0|0.8)$, and by factors $\{1.4, 1.5, 1.5\}$ in scenarios $\{\mathrm{A}, \mathrm{B}, \mathrm{C}\}$, respectively, for $(P_{e^+}|P_{e^-}) = (-0.3|0.9)$ compared to $(P_{e^+}|P_{e^-}) = (0|0.9)$. The signal to background ratio r is enhanced by $\{1.7, 1.7, 1.8\}$ for $(P_{e^+}|P_{e^-}) = (-0.3|0.8)$ compared to $(P_{e^+}|P_{e^-}) = (0|0.8)$ and by $\{1.4, 1.7, 1.8\}$ for $(P_{e^+}|P_{e^-}) = (-0.3|0.9)$ compared to $(P_{e^+}|P_{e^-}) = (0|0.9)$. If the positron beams would be polarized by $P_{e^+} = -60\%$, the enhancement factors for S are $\{2, 2.3, 2.4\}$, and for r they are $\{2.5, 3.2, 3.6\}$. For $P_{e^-} = 0.8$, it is only with positron polarization that we obtain values of r clearly above 1%. If we have $P_{e^-} = 0.9$, then r exceeds 1% without positron beam polarization.

Since the neutralinos are mainly bino, the signal cross section also depends sensitively on the mass $m_{\tilde{e}_{\rm R}}$ of the right selectron. In scenarios $\{\mathrm{A}, \mathrm{B}, \mathrm{C}\}$ the masses are $m_{\tilde{e}_{\rm R}} = \{133, 191, 261\}$ GeV, respectively; see Table 2. For larger masses, the signal to background ratio drops below $r < 1\%$. With $(P_{e^+}|P_{e^-}) = (-0.3|0.8)$, this happens for $m_{\tilde{e}_{\rm R}} = \{214, 300, 390\}$ GeV, and the significance would be $S < 5$. These selectron masses correspond to the mSUGRA parameter $M_0 = \{190, 270, 350\}$ GeV.

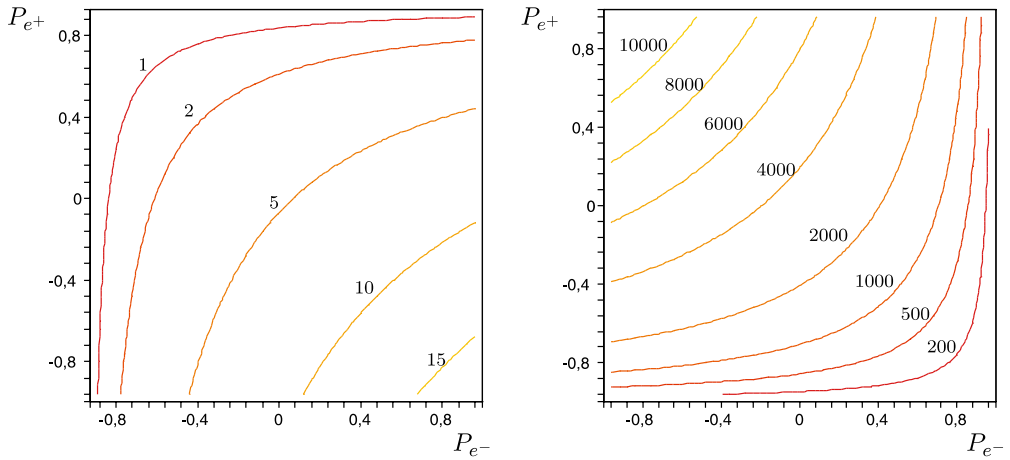

(a) Signal cross section $\sigma(e^+e^- \to \tilde{\chi}^0_1\tilde{\chi}^0_1\gamma)$ in fb.

(b) Background cross section $\sigma(e^+e^- \to \nu\bar{\nu}\gamma)$ in fb.

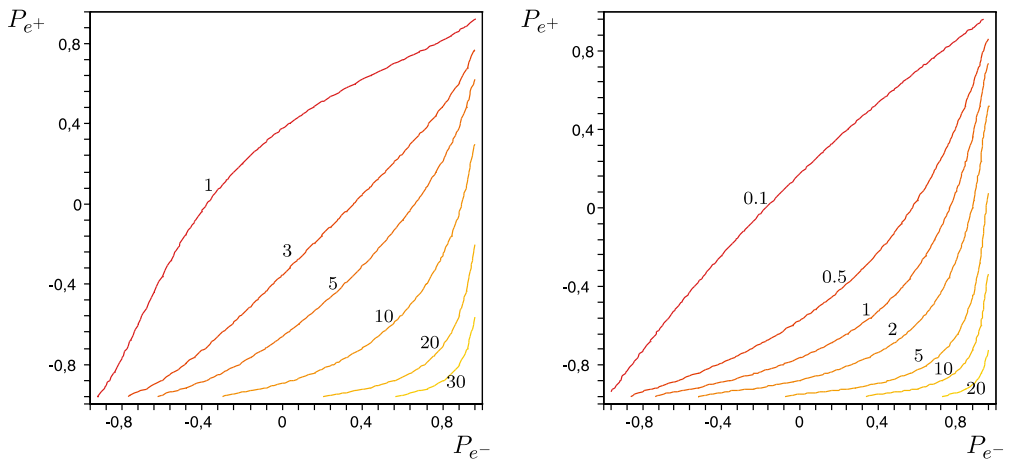

(c) Significance S.

(d) Signal to background ratio r in %.

Fig. 3. Signal cross section **a**, background cross section **b**, significance **c**, and signal to background ratio **d** for $\sqrt{s} = 500$ GeV, and an integrated luminosity $\mathcal{L} = 500\,\mathrm{fb}^{-1}$ for scenario C: $M_0 = 200$ GeV, $M_{1/2} = 415$ GeV, $A_0 = -200$ GeV, and $\tan\beta = 10$; see Tables 1 and 2

Table 3. Effective polarization $P_{\rm eff}$, cross sections σ, significance S, and signal to background ratio r for different beam polarizations $(P_{e^+}|P_{e^-})$ for scenario A at $\sqrt{s} = 220$ GeV, with $\mathcal{L} = 500\,\text{fb}^{-1}$

Scenario A	(0|0)	(0|0.8)	(−0.3|0.8)	(−0.6|0.8)	(0|0.9)	(−0.3|0.9)
$P_{\rm eff} = \frac{P_{e^-} - P_{e^+}}{1 - P_{e^-} P_{e^+}}$	0	0.8	0.89	0.95	0.9	0.94
$\sigma\big(e^+e^- \to \tilde{\chi}_1^0\tilde{\chi}_1^0\gamma\big)$	6.7 fb	12 fb	16 fb	19 fb	13 fb	16 fb
$\sigma(e^+e^- \to \nu\bar{\nu}\gamma)$	2685 fb	652 fb	534 fb	416 fb	398 fb	360 fb
S	2.9	10	15	20	14	19
r	0.3%	1.8%	2.9%	4.6%	3.2%	4.6%

Table 4. Effective polarization $P_{\rm eff}$, cross sections σ, significance S, and signal to background ratio r for different beam polarizations $(P_{e^+}|P_{e^-})$ for Scenario B at $\sqrt{s} = 350$ GeV, with $\mathcal{L} = 500\,\text{fb}^{-1}$

Scenario B	(0|0)	(0|0.8)	(−0.3|0.8)	(−0.6|0.8)	(0|0.9)	(−0.3|0.9)
$P_{\rm eff} = \frac{P_{e^-} - P_{e^+}}{1 - P_{e^-} P_{e^+}}$	0	0.8	0.89	0.95	0.9	0.94
$\sigma\big(e^+e^- \to \tilde{\chi}_1^0\tilde{\chi}_1^0\gamma\big)$	5.5 fb	9.6 fb	13 fb	15 fb	10.2 fb	13.3 fb
$\sigma(e^+e^- \to \nu\bar{\nu}\gamma)$	3064 fb	651 fb	481 fb	312 fb	350 fb	272 fb
S	2.2	8.4	13	19	12	18
r	0.2%	1.5%	2.6%	4.9%	2.9%	4.9%

Table 5. Effective polarization $P_{\rm eff}$, cross sections σ, significance S, and signal to background ratio r for different beam polarizations $(P_{e^+}|P_{e^-})$ for scenario C at $\sqrt{s} = 500$ GeV, with $\mathcal{L} = 500\,\text{fb}^{-1}$

Scenario C	(0|0)	(0|0.8)	(−0.3|0.8)	(−0.6|0.8)	(0|0.9)	(−0.3|0.9)
$P_{\rm eff} = \frac{P_{e^-} - P_{e^+}}{1 - P_{e^-} P_{e^+}}$	0	0.8	0.89	0.95	0.9	0.94
$\sigma\big(e^+e^- \to \tilde{\chi}_1^0\tilde{\chi}_1^0\gamma\big)$	4.7 fb	8.2 fb	11 fb	13 fb	8.6 fb	11.2 fb
$\sigma(e^+e^- \to \nu\bar{\nu}\gamma)$	3354 fb	689 fb	495 fb	301 fb	356 fb	263 fb
S	1.8	7	11	17	10	15
r	0.1%	1.2%	2.2%	4.4%	2.4%	4.3%

Note on wino- and higgsino-like neutralinos

In anomaly mediated supersymmetry breaking (AMSB) scenarios, the gaugino mass parameters are roughly related by $M_1 \approx 2.8 M_2$ at the weak scale [34]. As a consequence, the lightest neutralino is wino-like, and left slepton exchange is enhanced in the reaction $e^+e^- \to \tilde{\chi}_1^0\tilde{\chi}_1^0\gamma$. Therefore, it is no longer possible to increase the signal and to reduce the background simultaneously by a suitable choice of beam polarizations. In AMSB scenarios, also $m_0 \gtrsim 400$ GeV is bounded from below [35] and rather large. For smaller m_0, either the lightest stau is the LSP or sleptons would already have been observed. The relatively heavy selectrons lead then to a suppression of the cross section for radiative neutralino production. For example in the scenario SPS9 [27, 28] with $m_0 = 450$ GeV and $m_{\tilde{e}_{\rm L}} = 387$ GeV, $m_{\tilde{e}_{\rm R}} = 375$ GeV, $m_{\tilde{\tau}_1} = 349$ GeV, calculated with SPheno [32], we find that the significance is $S < 1$ and the signal to background ratio $r < 0.03\%$, for various values of the beam polarizations at $\sqrt{s} = 500$ GeV. Finally, in AMSB scenarios the lightest neutralino $\tilde{\chi}_1^0$ is nearly mass degenerate with the lightest chargino $\tilde{\chi}_1^\pm$. Thus, if the radiative production of neutralinos is kinematically accessible, also the pair production of charginos $e^+e^- \to \tilde{\chi}_1^+\tilde{\chi}_1^-$ can be well observed. In this context it is interesting to note that the radiative production of charginos $e^+e^- \to \tilde{\chi}_1^+\tilde{\chi}_1^-\gamma$ might be important, if the charginos decay almost invisibly [36]. This could happen if the neutralino–chargino mass difference is such that the charginos decay into rather soft pions, $\tilde{\chi}_1^\pm \to \tilde{\chi}_1^0\pi^\pm$.

The cross section of radiative neutralino production is also small in models, where the lightest neutralino is higgsino-like, i.e. $\mu \ll M_2$. For example, for $\mu < 300$ GeV and $M_2 > 500$ GeV we find $S < 1$ and $\sigma\big(e^+e^- \to \tilde{\chi}_1^0\tilde{\chi}_1^0\gamma\big) < 1$ fb, since the gaugino couplings of the neutralino are suppressed. The couplings of the neutralino to the Z boson are proportional to the squared difference of the higgsino couplings, $|N_{13}|^2 - |N_{14}|^2$ [18], and thus too small to lead to an observable signal.

4 Summary and conclusions

We have studied radiative neutralino production $e^+e^- \to \tilde{\chi}_1^0\tilde{\chi}_1^0\gamma$ at the ILC with longitudinally polarized beams. For the center-of-mass energies $\sqrt{s} = 220\,\text{GeV}$, 350 GeV, and 500 GeV, we have considered three specific mSUGRA inspired scenarios. In our scenarios, only radiative neutralino production is kinematically accessible, since the other supersymmetric particles are too heavy to be pair produced. We have investigated the beam polarization dependence of the cross section from radiative neutralino production and the background form radiative neutrino production $e^+e^- \to \nu\bar{\nu}\gamma$.

We have shown that polarized beams enhance the signal and suppress the background simultaneously and significantly. In our scenarios, the signal cross section for $(P_{e^+}|P_{e^-}) = (-0.3|0.8)$ is larger than 10 fb, the significance $S > 10$, and the signal to background ratio is about 2%–3%. The background cross section can be reduced to 500 fb. Increasing the positron beam polarization to $P_{e^+} = -0.6$, both the signal cross section and the significance increase by about 25%, in our scenarios. For $(P_{e^+}|P_{e^-}) = (0.0|0.9)$ the radiative neutralino production signature is observable at the ILC but both the significance and the signal to background ratio are considerable improved for $(P_{e^+}|P_{e^-}) = (-0.3|0.9)$, making more detailed investigations possible. The electron and positron beam polarization at the ILC are thus essential tools to observe radiative neutralino production. For unpolarized beams this process cannot be measured.

We conclude that radiative neutralino production can and should be studied at $\sqrt{s} = 500\,\text{GeV}$, as well as at the lower energies $\sqrt{s} = 220\,\text{GeV}$ and $\sqrt{s} = 350\,\text{GeV}$, which are relevant for Higgs and top physics. We have shown that for these energies there are scenarios, where other SUSY particles like heavier neutralinos, charginos and sleptons are too heavy to be pair produced. In any case, a pair of radiatively produced neutralinos is the lightest accessible state of SUSY particles to be produced at the linear collider.

Acknowledgements. We would like to thank Gudrid Moortgat-Pick and Klaus Desch for very helpful discussions. This work was supported by the SFB Transregio 33: The Dark Universe. One of us (OK) would like to thank the organizers of the ECFA-ILC workshop Valencia 06, where the initial idea for this work was developed.

References

1. H.P. Nilles, Phys. Rep. **110**, 1 (1984)
2. H.E. Haber, G.L. Kane, Phys. Rep. **117**, 75 (1985)
3. M. Drees, hep-ph/9611409
4. I.J.R. Aitchison, hep-ph/0505105
5. LHC/LC Study Group, G. Weiglein et al., hep-ph/0410364
6. A. Djouadi, J. Lykken, K. Mönig, Y. Okada, M.J. Oreglia, S. Yamashita, International Linear Collider Reference Design Report Volume 2: PHYSICS AT THE ILC arXiv:0709.1893 [hep-ph]
7. ECFA/DESY LC Physics Working Group, J.A. Aguilar-Saavedra et al., hep-ph/0106315
8. American Linear Collider Working Group, T. Abe et al., hep-ex/0106055
9. ACFA Linear Collider Working Group, K. Abe et al., hep-ph/0109166
10. G.A. Moortgat-Pick et al., hep-ph/0507011; http://www.ippp.dur.ac.uk/∼gudrid/source/
11. Summary talk of the polarization parallel session by S. Riemann given at the ILC conference in Valencia, 5–13 November 2006, http://ific.uv.es/ ilc/ECFA-GDE2006/
12. Talk by G. Moortgat-Pick in the polarization parallel session at the ILC conference in Valencia, 5–13 November 2006, http://ific.uv.es/ ilc/ECFA-GDE2006/
13. Talk by E Reinherz-Aronis in the polarization parallel session at the ILC conference in Valencia, 5–13 November 2006, http://ific.uv.es/ ilc/ECFA-GDE2006/
14. G. Moortgat-Pick, hep-ph/0607173
15. A. Datta, A. Datta, S. Raychaudhuri, Phys. Lett. B **349**, 113 (1995) [hep-ph/9411435]
16. A. Datta, A. Datta, S. Raychaudhuri, Eur. Phys. J. C **1**, 375 (1998) [hep-ph/9605432]
17. S. Ambrosanio, B. Mele, G. Montagna, O. Nicrosini, F. Piccinini, Nucl. Phys. B **478**, 46 (1996) [hep-ph/9601292]
18. H.K. Dreiner, O. Kittel, U. Langenfeld, Phys. Rev. D **74**, 115 010 (2006) [hep-ph/0610020]
19. S.Y. Choi, J.S. Shim, H.S. Song, J. Song, C. Yu, Phys. Rev. D **60**, 013 007 (1999) [hep-ph/9901368]
20. H. Baer, A. Belyaev, in Proc. of the APS/DPF/DPB Summer Study on the Future of Particle Physics (Snowmass 2001) ed. by N. Graf, eConf **C010 630**, P336 (2001) [hep-ph/0111017]
21. A.H. Chamseddine, R. Arnowitt, P. Nath, Phys. Rev. Lett. **49**, 970 (1982)
22. P. Nath, R. Arnowitt, A.H. Chamseddine, Nucl. Phys. B **227**, 121 (1983); for a review see also [1].
23. M.T. Dova, P. Garcia-Abia, W. Lohmann, hep-ph/0302113
24. Particle Data Group, W.M. Yao et al., J. Phys. G **33**, 1 (2006)
25. I. Borjanovic et al., Eur. Phys. J. C **39S2**, 63 (2005) [hep-ex/0403021]
26. M. Martinez, R. Miquel, Eur. Phys. J. C **27**, 49 (2003) [hep-ph/0207315]
27. J.A. Aguilar-Saavedra et al., Eur. Phys. J. C **46**, 43 (2006) [hep-ph/0511344]
28. B.C. Allanach et al., in Proc. of the APS/DPF/DPB Summer Study on the Future of Particle Physics (Snowmass 2001) ed. by N. Graf, Snowmass, Colorado, 30 June–21 July 2001 [hep-ph/0202233]
29. M. Dittmar, H.K. Dreiner, Phys. Rev. D **55**, 167 (1997) [hep-ph/9608317]
30. M. Dittmar, H.K. Dreiner, hep-ph/9703401
31. N. Ghodbane, H.U. Martyn, in Proc. of the APS/DPF/DPB Summer Study on the Future of Particle Physics (Snowmass 2001) ed. by N. Graf, hep-ph/0201233
32. W. Porod, Comput. Phys. Commun. **153**, 275 (2003) [hep-ph/0301101]
33. T. Omori, KEK-PREPRINT-98-237, presented at the 1st ACFA Workshop on Physics Detector at the Linear Collider, Beijing, China, 26–28 November 1998

34. M. Drees, R. Godbole, P. Roy, Theory and phenomenology of sparticles: An account of four-dimensional $N = 1$ supersymmetry in high energy physics (World Scientific, Hackensack, USA, 2004)
35. See, e.g., A. Datta, A. Kundu, A. Samanta, Phys. Rev. D **64**, 095 016 (2001) [hep-ph/0101034]
36. A. Datta, S. Maity, Phys. Lett. B **513**, 130 (2001) [hep-ph/0104086]